BIOCHEMISTRY
including biophysical chemistry & molecular biology

Article

pubs.acs.org/biochemistry

Single-Molecule Studies of the Lysine Riboswitch Reveal Effector-Dependent Conformational Dynamics of the Aptamer Domain

Larry R. Fiegland,[†,‡] Andrew D. Garst,[†] Robert T. Batey,[†] and David J. Nesbitt*[,†,‡]

[†]Department of Chemistry and Biochemistry and [‡]JILA, National Institute of Standards and Technology, University of Colorado, Boulder, Colorado 80309, United States

Supporting Information

ABSTRACT: The lysine riboswitch is a cis-acting RNA genetic regulatory element found in the leader sequence of bacterial mRNAs coding for proteins related to biosynthesis or transport of lysine. Structural analysis of the lysine-binding aptamer domain of this RNA has revealed that it completely encapsulates the ligand and therefore must undergo a structural opening/closing upon interaction with lysine. In this work, single-molecule fluorescence resonance energy transfer (FRET) methods are used to monitor these ligand-induced structural transitions that are central to lysine riboswitch function. Specifically, a model FRET system has been developed for characterizing the lysine dissociation constant as well as the opening/closing rate constants for the *Bacillus subtilis lysC* aptamer domain. These techniques permit measurement of the dissociation constant (K_D) for lysine binding of 1.7(5) mM and opening/closing rate constants of 1.4(3) s^{-1} and 0.203(7) s^{-1}, respectively. These rates predict an apparent dissociation constant for lysine binding ($K_{D,apparent}$) of 0.25(9) mM at near physiological ionic strength, which differs markedly from previous reports.

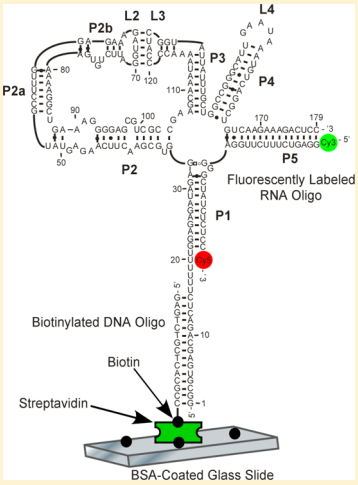

A broad array of noncoding RNAs and RNA elements control a significant amount of normal cellular metabolism in all kingdoms of life.[1−3] One of the more recently discovered classes of noncoding RNA elements in bacteria are riboswitches. These regulatory elements are found in the leader sequence of mRNAs and control gene expression by directly binding a specific small molecule, which in turn directs a secondary structural switch that coordinates with the expression machinery.[4,5] Currently, over 20 biochemically validated classes of riboswitches that bind a broad range of ligands including amino acids,[6,7] metal ions,[8] vitamin cofactors,[9,10] purine nucleobases,[11,12] and amino sugars[13] have been identified. In *B. subtilis* and related *Firmicutes*, riboswitches are an important mechanism of regulation, playing a role in the regulation of at least 4% of all genes.[14] The unique nature of these regulatory elements and their involvement in regulation of genes essential to bacterial survival and/or virulence have made riboswitches potentially important targets for antimicrobial therapeutics.[15]

Riboswitches control gene expression through the interplay of two functional domains: (i) an *aptamer domain* that serves as a receptor for binding a specific effector ligand and (ii) the *expression platform*, which contains the secondary structural switch.[16,17] The currently accepted model for how riboswitches translate binding of ligand into a regulatory response is that binding of the effector to the aptamer stabilizes incorporation of a specific sequence element into the aptamer, thereby precluding formation of one of the two mutually exclusive secondary structures in the expression platform. One of the secondary structures in the expression platform is then used to direct the expression machinery. For example, within riboswitches that control transcription of the mRNA, one of these secondary structures is a rho-independent transcriptional terminator stem−loop that causes RNA polymerase to prematurely abort mRNA synthesis. The alternate secondary structure, the antiterminator stem−loop, allows the polymerase to proceed through the riboswitch and synthesize the entire message. Depending upon the nature of the expression platform, riboswitches can control expression at the transcription or translational level or by splicing in eukaryotic mRNAs.[5]

For riboswitches that control transcription, ligand binding must occur within a limited time window to elicit the appropriate regulatory response before the polymerase escapes the leader sequence.[16,18] As a consequence, rates of ligand binding, aptamer folding, and alternative secondary structure formation are kinetically critical determinants for the concentration range of the ligand that is required to elicit the regulatory response.[18] In addition to the kinetics of binding, the ability of the aptamer to rapidly and efficiently fold is also critical to the regulatory activity of transcriptional riboswitches. For example, a recent study by Greenleaf et al. applied single-

Received: June 11, 2012
Revised: September 6, 2012
Published: October 15, 2012

molecule force spectroscopy to study the kinetics of folding and ligand binding of the aptamer domain of an adenine binding riboswitch.[19] Their analysis yielded a rate constant of 0.4 s^{-1} for folding of a competent aptamer domain and k_{on} and k_{off} values of 8×10^4 M^{-1} s^{-1} and 0.2 s^{-1}, respectively, for ligand binding. For a typical intracellular concentration of adenine of 1.5 μM,[20] these rate constants translate into characteristic times of ≈2.5 s for folding, ≈8 s for ligand binding, and ≈5 s for ligand dissociation. These relatively slow rates suggest that both aptamer folding and ligand binding occur on a time scale similar to transcription of the riboswitch, which is on the order of ∼4−20 s for the transcription of 200 nucleotides.[21] This observation supports a hypothesis that the *individual rate constants* of folding and binding dictate the regulatory response in a subset of riboswitches rather than equilibrium thermodynamics,[19] a paradigm which is further supported by ensemble studies.[22]

To further examine these aspects of riboswitch function, we have analyzed the binding properties of the *B. subtilis lysC* riboswitch aptamer using single molecule fluorescence resonance energy transfer (smFRET) techniques. As shown in Figure 1a,b, the aptamer domain of all lysine riboswitches

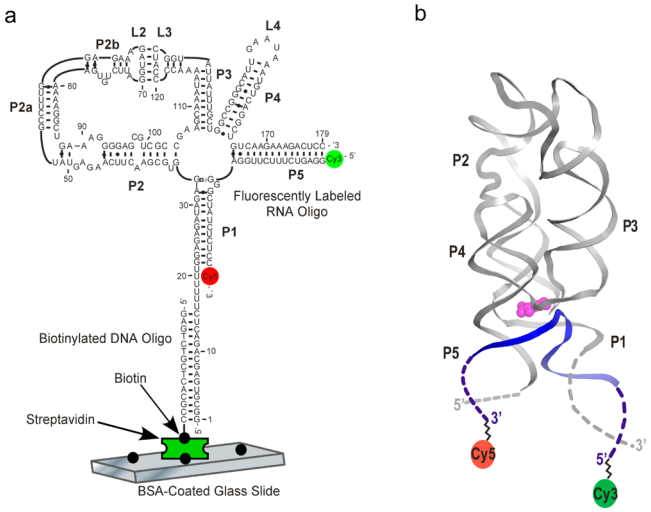

Figure 1. RNA construct for Cy3-Cy5 FRET-monitoring of the opening/closing induced by lysine binding to the riboswitch aptamer domain. (a) Secondary structure demonstrating hybridization of the 3′-biotin DNA strand to the RNA aptamer domain, which facilitates immobilization to a surface via interaction with streptavidin. (b) Crystal structure showing the tertiary interaction of the aptamer-binding domain with lysine (shown in magenta) bound. Fluorescently labeled RNA oligo is shown in blue.

consists of a five-way helical junction containing the lysine binding site.[7,23,24] The helices surrounding this junction are roughly organized into three coaxial stacks (P1/P2/P2a, P2b/P3, and P4/P5) whose arrangement is supported by long-range interactions involving the terminal loops L2, L3, and L4 (Figure 1a,b).[25,26] This conformation results in close juxtaposition of the P1 and P5 helices as observed in the crystal structure (Figure 1b), a placement that may be of functional significance since the P1 helix participates in forming alternative secondary structures with the expression platform. Indeed, recent FRET measurements and mutational analysis at the ensemble level indicate that the appropriate positioning of these helices is required for transcriptional regulation *in vitro*.[27]

In the present study, we have developed a model single-molecule system to characterize the conformational changes experienced by the *Bacillus subtilis lysC* aptamer domain upon ligand binding as well as to measure the kinetics of this interaction. Specifically, we exploit multiple ensemble and single-molecule fluorescence resonance energy transfer (FRET) methods for real-time studies of folding transitions central to riboswitch function. Of special relevance, the single-molecule FRET techniques provide us with both spatial and temporal information on the conformational changes, allowing us to measure the individual opening and closing rate constants induced by lysine binding. In particular, this overall combination of multiple (e.g., ensemble, confocal, and wide-field TIRF) FRET methods allows us to access a wide range of kinetic time scales from milliseconds to minutes and thereby isolate unique subpopulations related to the folding transitions induced by lysine binding.

MATERIALS AND METHODS

A modified three-piece *B. subtilis lysC* aptamer construct has been developed (see Figure 1a), with a doubly, fluorescently labeled section for FRET reporting on conformational changes induced by lysine binding to the aptamer-binding domain. Fluorescence studies exploiting (i) ensemble, (ii) single molecule confocal, and (iii) single molecule wide-field TIRF techniques are explored, under buffer conditions (50 mM HEPES, pH 7.5, 100 mM NaCl, 50 mM KCl, 0.10 mM EDTA, and 1 mM $MgCl_2$) containing an enzymatic oxygen scavenging system (protocatechuic acid/protocatechuate-3,4-dioxygenase) and a triplet-state quencher (6-hydroxy-2,5,7,8-tetramethyl-chroman-2-carboxylic acid).[28,29] For the single molecule confocal and wide-field TIRF studies, the construct includes a sequence in the P1 stem region that can hybridize to a short strand of biotinylated DNA and thereby permit tethering to the coverslip surface via biotin−streptavidin chemistry. Further details pertaining to (i) synthesis of the riboswitch aptamer-binding construct, (ii) experimental apparatus used in this study, (iii) fluorescence techniques, and (iv) data analysis are provided in the Supporting Information.

RESULTS

A. Lysine-Induced Conformational Change of the *lysC* Aptamer Domain. Chemical probing experiments of several lysine riboswitch aptamer domains have shown that the five-way helical junction experiences a local structural change upon ligand binding.[7,25] In contrast, X-ray crystal structures and small-angle X-ray scattering (SAXS) analysis suggest that the structure of the RNA does not change substantially between its unliganded and liganded forms.[25,26,30] However, any lysine-induced conformational change in the RNA most likely involves a change in the orientation of the P1 and P5 helices relative to one another, due to local changes in the five-way junction upon lysine binding.[25,27] In order to have the greatest sensitivity to such lysine-specific structural rearrangements, we therefore have attached Cy3 and Cy5 fluorophores to the distal ends of the P1 and P5 helices, respectively. In addition, we have also extended the helices to accommodate fluorescence labeling as well as to enhance annealing efficiency of the three-strand construct (see Figure 1a). It is worth noting that this strategy is quite similar to the labeling scheme used in a previous lysine riboswitch study at the ensemble level, specifically for

dx.doi.org/10.1021/bi3007753 | *Biochemistry* 2012, 51, 9223−9233

investigating conformational changes induced by divalent metal ions.[27]

We first consider FRET studies at the ensemble level. As shown in Figure 2a, lysine binding to the aptamer domain does indeed alter the relative orientation of the P1 and P5 helices. This motion changes the distance between the fluorophores attached to the fluorescently labeled RNA oligonucleotide, which translates into a conventional FRET modulation signal between donor and acceptor dyes. It is important to note, however, that previous reports reveal dissociation constants for ligand binding to various RNA aptamers to be highly dependent upon magnesium concentration.[31−33] Thus, we choose to work under approximately physiological magnesium conditions (1 mM) in order to determine both dissociation constants and kinetic rate constants that are physiologically relevant.[34−38] When fluorescence spectra are recorded as a function of lysine concentration, strong FRET signals are observed, as shown by an increase in acceptor (Cy5) and a corresponding decrease in donor (Cy3) fluorescence.

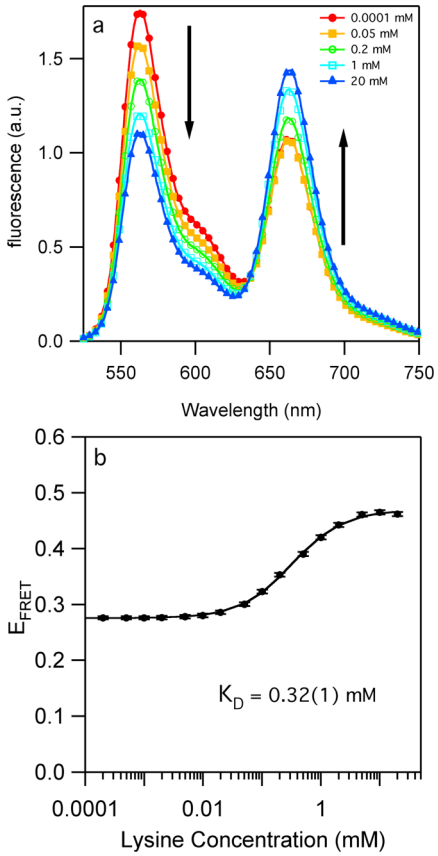

Figure 2. Lysine-induced folding of the riboswitch aptamer domain. (a) Ensemble fluorescence spectra at lysine concentration between 0.0001 and 20 mM, with fluorescence excited at 500 nm. The fluorescence between 525 and 600 nm is primarily from Cy3 fluorophore, whereas emission greater than 640 nm is from the Cy5 fluorophore. Arrows indicate direction of change of the donor and acceptor regions of the spectra as the lysine concentration increases. (b) Ensemble FRET measurements of the conformational changes of the riboswitch construct induced by lysine.

A small sampling of the total set of spectra taken over a series of lysine concentrations is shown in Figure 2a; most importantly, the spectra demonstrate a clear isoemmissive point. In the simplest kinetic modeling, this behavior would be consistent with a two-state system described by

$$\text{RNA} + \text{lysine} \underset{k_2}{\overset{k_1}{\rightleftarrows}} \text{RNA·lysine} \quad (1)$$

which yields the energy transfer efficiency (E_{FRET}) as a function of lysine concentration shown in Figure 2b. In the context of this simplified two-state binding model, the experimental E_{FRET} values can be generally fit to

$$E_{FRET}([\text{lysine}]) = E_i + (\Delta E)\left(\frac{[\text{lysine}]^n}{K_{D,\text{lysine}}{}^n + [\text{lysine}]^n}\right) \quad (2)$$

where E_i is the FRET efficiency in the absence of lysine, ΔE is the asymptotic change in FRET under saturating lysine conditions, n is the Hill coefficient, and $K_{D,\text{lysine}}$ is the apparent dissociation constant. Least-squares fits of the ensemble FRET data to eq 2 yield E_i = 0.275(7), ΔE = 0.194(2), and n = 1.00(3), with a value for $K_{D,\text{lysine}}$ = 0.32(1) mM, which is nearly *1000-fold greater* (i.e., less sensitive) than previous lysine dissociation constants reported in the literature.[26,39] Quite relevantly, this is the first reported measurement of the K_D for the lysine metabolite under physiologically relevant magnesium conditions. This proves to be critical, as it has been shown for other aptamer domains that the ligand binding affinity increases dramatically with magnesium concentration.[31−33] Interestingly, K_D values at near 0.3−0.4 mM levels obtained under physiological Mg^{2+} conditions are in fact already quite comparable with typical intracellular concentrations of lysine (0.41 mM) in glucose-fed, exponentially growing *E. coli*.[20] Thus, the current K_D value may therefore be entirely consistent with riboswitch function as a sensor for intracellular lysine. Most of all, these data provide the first clear evidence that lysine binding *by itself* specifically influences the global conformation of the lysine riboswitch, rather than promotion of RNA folding solely by addition of magnesium.[27] High sensitivity of ligand binding and catalytic function to Mg^{2+} concentration for riboswitches has been previously observed and is discussed in more detail in the Discussion section.

To further explore the sensitivity of ligand binding to the Mg^{2+} concentration for the lysine riboswitch, we recorded ensemble fluorescence spectra as a function of lysine concentration at numerous Mg^{2+} concentrations. The FRET efficiencies determined from theses spectra are shown as a function of lysine in Figure S3 of the Supporting Information. From this data it is clearly evident that as the Mg^{2+} concentration increases, the apparent lysine dissociation constant decreases. By examining the far left side of the graph, the data also suggest that the lysine riboswitch can fold in the absence of ligand. This is observed by the increase in FRET efficiency for the ensemble data as the Mg^{2+} concentration is increased. This observation is consistent with a previous lysine riboswitch study at the ensemble level, which specifically investigated conformational changes induced by divalent metal ions.[27] It is interesting to note that this study observed small changes in FRET efficiency with and without ligand at low Mg^{2+} concentration (<1 mM), but the authors did not observe changes in the FRET efficiency with and without ligand at high Mg^{2+} concentration (>1 mM). The data presented in Figure S3 clearly demonstrates a change in the FRET efficiency with and without ligand even at elevated Mg^{2+} concentrations (10 mM). The discrepancy between these two separate experiments can be explained by differences in the

dx.doi.org/10.1021/bi3007753 | *Biochemistry* 2012, 51, 9223−9233

fluorophore labeling efficiency of the two unique constructs. The average FRET efficiency is easily influenced by molecules containing only the donor fluorophore and is therefore highly dependent upon experimental conditions during the synthesis of the riboswitch construct.

To ensure that the placement of the fluorophores within the construct or synthetic procedures used to produce the riboswitch construct did not significantly influence the dissociation constant of lysine binding, we performed controlled experiments in which we measure the dissociation constant of the wild-type *Bacillus subtilis lysC* aptamer domain using isothermal titration calorimetry (ITC), data shown in Figure S4 of the Supporting Information. Figure S4 also compares the ITC measurements of the wild-type *Bacillus subtilis lysC* aptamer domain to the apparent dissociation constants measured from the fluorescently labeled riboswitch using ensemble FRET techniques. Both experimental techniques reveal that the apparent dissociation constant is highly sensitive to the Mg^{2+} concentration with the apparent dissociation constant decreasing as the Mg^{2+} concentration is increased. There are slight differences noticed between the sensitivity to Mg^{2+} concentration between the fluorescently labeled construct and the wild-type construct (see Figure S4) with the fluorescently labeled construct requiring slightly more magnesium to achieve the same response as the wild-type construct. The fluorescent-labeling of the riboswitch could cause these small discrepancies, but these differences can be more likely attributed to the fact that we have extended the P1 and P5 helices to accommodate fluorescence labeling as well as to enhance annealing efficiency of the three-strand construct. This extension would require slightly more magnesium to effectively screen all the negative charges of the phosphate backbone. These experiments reveal an apparent dissociation constant for lysine binding of 0.056(9) mM at a physiologically relevant Mg^{2+} concentration of 1 mM for the wild-type construct. Since the observed dissociation constant for lysine binding for the wild-type riboswitch is ~6× greater than the fluorescently labeled riboswitch's dissociation constant, 0.32(1) mM, we conclude that the placement of the fluorophores or synthetic procedures used to synthesize our riboswitch construct did influence the apparent dissociation constant, but the observed trends, high sensitivity to the magnesium concentration, are consistent between both constructs. Although there are small differences between the wild-type construct and fluorescently labeled construct, the fluorescently label construct allows us to further probe the riboswitch in ways that are not possible with the native structure. In addition to ensemble binding properties, the fluorescently labeled construct allows us to investigate the kinetics of the RNA folding process in addition to the ligand binding equilibrium.

B. Freely Diffusing Single Molecule Burst Measurements. Since bulk fluorescent ensemble methods can be influenced by a number of experimental artifacts (i.e., single-labeled constructs, misfolded states, presence of free dye in solution, heterogeneous labeling, etc.), we tested the above ensemble fluorescence measurements more rigorously by also pursuing single molecule burst studies of freely diffusing constructs. These measurements, in principle, can offer important insight into the "open" vs "closed" conformations and populations of the lysine riboswitch aptamer. Specifically, burst fluorescence methods have been used to quantify the population distributions observed at a given E_{FRET} level, taking critical advantage of clever alternating-laser excitation (ALEX) methods of Weiss and co-workers to unambiguously confirm the presence of doubly labeled constructs (see Supporting Information for details). Sample histograms for the resulting open and closed populations as a function of increasing lysine concentration are shown in Figure 3a. As expected, a lysine-induced conformational change is signaled by a peak at higher FRET efficiency that grows in with higher lysine concentration, with a simultaneous decrease in the distribution of open riboswitches with lower E_{FRET} values.

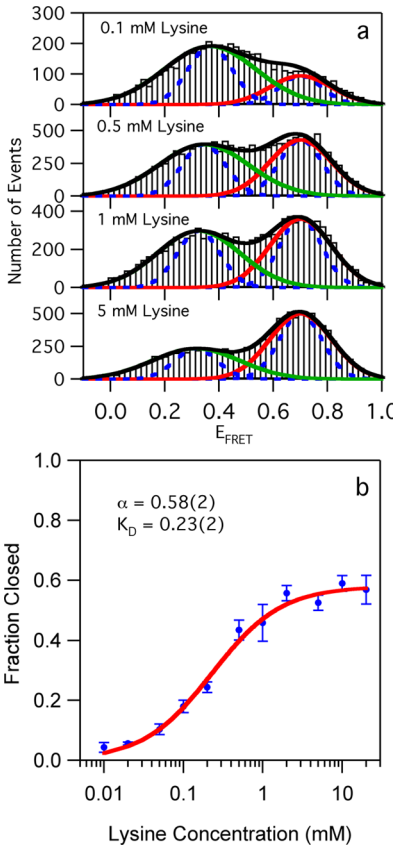

Figure 3. Sample single-molecule data analysis of freely diffusing lysine riboswitch constructs. (a) E_{FRET} population histograms as a function of [lysine] with fits to the sum of two Gaussian distributions superimposed (black line). The individual Gaussian components reveal distinct populations of opened (green) and closed (red) constructs. Dashed blue line represents shot-noise limited line-shape predictions. Lysine induces folding of the riboswitch construct, as evidenced by the shift in the relative population from the opened (low E_{FRET}) to closed (high E_{FRET}) states. (b) Least-squares fits of the fraction of closed molecules ($f = N_{closed}/(N_{closed} + N_{opened})$) versus [lysine] to eq 3.

To more quantitatively investigate the fraction of burst events corresponding to a given subpopulation, the full set of E_{FRET} histograms at different lysine concentrations has been simultaneously fit to a two Gaussian distribution. The peak widths and centers for the closed conformer subpopulation are treated as common but adjustable parameters, with the corresponding values for the open conformer subpopulations floated for each lysine concentration. Fractional populations of open verses closed aptamer binding conformations are then determined[40−42] by $f = N_{closed}/(N_{closed} + N_{open})$, where N_{closed} and N_{open} represent integrated areas of the closed and open Gaussian peaks. As demonstrated in Figure 3b, the fraction of

dx.doi.org/10.1021/bi3007753 | *Biochemistry* 2012, 51, 9223−9233

closed molecules rises monotonically with increasing lysine concentration but reaches an asymptotic value less than unity under saturating conditions.

Based on the simple kinetic model in eq 1, the lysine-dependent fraction of closed riboswitch conformers can be fit (solid red line, Figure 3b) to a standard Hill binding equation

$$f = \frac{\alpha[\text{lysine}]^n}{K_D{}^n + [\text{lysine}]^n} \quad (3)$$

with the modification that only a finite fraction ($\alpha < 1$) of the molecules achieve the closed conformation upon binding lysine. For a Hill coefficient $n \approx 1$, the fit yields an independent second estimate for the apparent dissociation constant, K_D = 0.23(2) mM, which agrees relatively well with the apparent K_D measured with ensemble fluorescence methods discussed above. Additionally, these burst measurements indicate that only α = 58(2)% of the doubly labeled constructs diffusing through the confocal volume close upon lysine binding. One interpretation would be that the remaining ≈42% population minority is trapped in an inactive conformation in which the ligand-binding pocket is misfolded as a result of the annealing procedure. However, an alternate interpretation would be that the simple two-state model (eq 1) is insufficient to describe structural changes induced by lysine binding. The model would have to be expanded to at least three states to accommodate the data, a topic to which we return later.

Analysis of the distribution widths in Figure 3a provides further information on conformational dynamics of the open and closed subpopulations. The dashed blue lines in Figure 3a represent shot-noise limited behavior, where the width reflects finite photon statistics for donor and acceptor. This shot-noise broadening is defined by $\sigma_{SN} = (\langle E_{FRET}\rangle(1 - \langle E_{FRET}\rangle)/T)^{1/2}$, where $\langle E_{FRET}\rangle$ is the average efficiency of energy transfer and T is the photon threshold for event identification.[41] Gaussian fits to these histograms yield peak widths for open and closed populations that are 2.1(1) and 1.46(1) times the shot-noise limit, respectively. There are many other possible sources of E_{FRET} broadening, including spectral diffusion, hindered rotational motion, and/or quantum-yield fluctuation of the dye labels. Fortunately, each of these sources have been studied extensively and ruled out by Antonik et al.[28,42] as likely broadening mechanisms for Alexa-488-Cy5 FRET pairs, with comparable behavior expected for Cy3-Cy5. Instead, broadening of these distributions in excess of shot-noise more likely reflects a dynamical distribution of closed or open states, each with multiple conformations with similar but experimentally unresolved FRET efficiencies.

C. Raster-Scanned FRET Images. Considerably more quantitative information on both the kinetics and equilibrium properties of the riboswitch aptamer-binding domain can be obtained by observing lysine-induced structural changes *in real time* for single molecule constructs tethered to a surface by biotin−strepavidin chemistry. On the outset, however, we must first verify that surface immobilization does not perturb the equilibrium distribution and associated FRET states for the closed and open subpopulations. In order to achieve this, raster-scanned single-molecule ALEX fluorescence images have been collected for surface-tethered lysine riboswitch constructs, under both (i) "zero" lysine [0 mM] and (ii) "high" lysine [20 mM] conditions. Specifically, we exploit a microfluidic flow cell to permit imaging of the same riboswitch constructs under (i) two-color alternating laser excitation (ALEX) of donor (Figure 4a,b) and acceptor (Figure 4c,d) fluorophores and (ii) low (0 mM) and high (20 mM) lysine conditions promoting

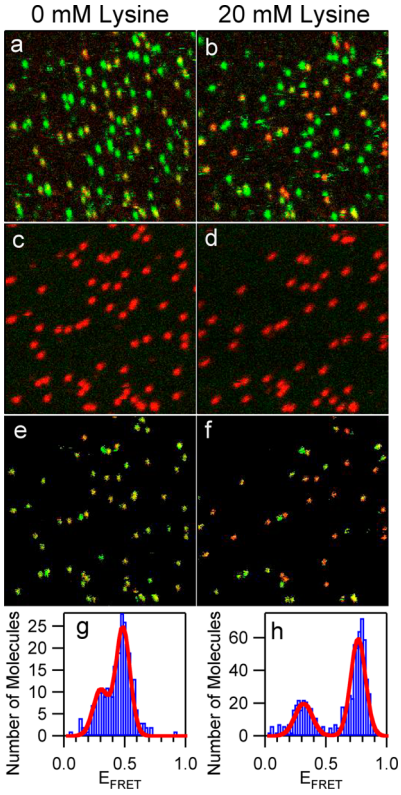

Figure 4. Representative single-molecule raster-scanned images and analysis of the lysine riboswitch construct at no (0 mM) and high (20 mM) lysine conditions. Images are plotted in false color with donor fluorescence in green and acceptor fluorescence in red. Each image is 12.5 × 12.5 μm. The same riboswitch molecules are being observed in each image. (a, b) Fluorescence images collected during the donor excitation period under conditions with no lysine and high lysine, respectively. (c, d) Fluorescence images collected during the acceptor excitation period under conditions of no lysine and high lysine, respectively. (e, f) ALEX filtered fluorescence images measured under conditions of no lysine and high lysine, respectively. (g, h) Corresponding histograms of the average E_{FRET} of each molecule for 0 mM lysine (g) and 20 mM lysine (h) conditions. The histograms are superimposed with fits to a sum of two Gaussian distributions (solid red line).

open and closed conformations (Figure 4e,f). In analogy with the freely diffusing burst fluorescence methods, a dual-threshold analysis of the two-color signals is employed to generate ALEX filtered raster scan images composed of only riboswitch constructs that contain both donor and acceptor fluorophores.

Addition of lysine (20 mM) to the microfluidic samples yields a clear increase in FRET efficiency, as demonstrated by change in the false color ALEX images from orange (Figure 4e) to red (Figure 4f). This increase in FRET efficiency signals a conformational change in which the P1 and P5 helices are brought closer together, most likely by a decrease in the P1/P5 interhelical angle. Furthermore, the FRET efficiency values and distributions from these raster-scanned ALEX images provide evidence for constructs existing in three distinct conformational subpopulations. In the absence of lysine (left panels), for example, molecules with both active donor and acceptor fluorophores yield a histogram with two distinct subpopulations

dx.doi.org/10.1021/bi3007753 | *Biochemistry* 2012, 51, 9223−9233

(Figure 4g), which can be least-squares fit to two Gaussian peaks yielding E_{FRET} values of 0.29(2) and 0.474(8). The Gaussian peak component centered at the lower E_{FRET} = 0.29(2) value indicates a subset of molecules that *do not bind lysine* even under high lysine conditions, as can be seen by comparing the panels in Figure 4g,h. This subpopulation comprise 29(6)% of the total population. It is this subpopulation that is observed in the freely diffusing studies, which contributes to the width that is >2 times the shot-noise limit for the opened riboswitch populations. The experimental resolution for the freely diffusing burst measurements was not sufficient enough to uniquely isolate this subpopulation, but the experimental resolution for these raster-scanned images is clearly sufficient to isolate this subpopulation. The peak centered at E_{FRET} of 0.474(8) reflects the subset of molecules competent to access the closed conformation upon binding lysine, but which remains open under zero lysine conditions.

Under high lysine conditions (20 mM), a third population is observed with an E_{FRET} of 0.754(5) (Figure 4h). In this experiment, the RNA is actively switching between closed and opened conformations in the 4 min time scale over which these raster scanned images are collected. Thus, active molecules will result in a single peak with an E_{FRET} value corresponding to a population-weighted average of the closed and opened configurations. Since the molecules are spending most of their time in the closed conformation at high lysine conditions, this average E_{FRET} value is observed at 0.754(5). At high lysine concentration, we also see a subpopulation of molecules that do not fold on the time scale of the raster-scanned ALEX filtered image. This subpopulation comprises 28(4)% of the total and has an average E_{FRET} of 0.306(8), in excellent agreement with the E_{FRET} = 0.29(2) subpopulation values already noted in Figure 4g in the absence of lysine. One simple interpretation of these results would be that these riboswitch construct molecules have an inactive conformation of the ligand binding-pocket that prevents the binding of lysine and thus remain in a perpetually opened state. It is interesting to note that different RNA constructs, which are not riboswitches, studied in our laboratories also indicate a similar 30−35% of molecules that do not actively fold on the time scale of the experiments.[43] The raster-scanned images provided the resolution that was need to uniquely isolate this subpopulation of molecules.

D. Single-Molecule Binding Kinetics. The ensemble, freely diffusing single molecule burst fluorescence, and tethered single molecule ALEX raster scanned experiments described above provide considerable information regarding the conformational states of the RNA under various conditions. However, it is the time scale with which the RNA interconverts between these states that is relevant to riboswitch kinetics and defines the probability of a particular regulatory outcome. In order to determine rate constants for lysine-induced closing/opening, FRET trajectories of single tethered constructs have been acquired via total internal reflection fluorescence (TIRF) microscopy as a function of time and lysine concentration. FRET trajectories (data not shown) were originally measured on the confocal single molecule microscope used in the ALEX raster-scanned image experiments described above. Since the faster time resolution of the confocal experiments was not needed for the slow conformational changes (seconds) observed for this riboswitch, further FRET trajectories were obtained using TIRF microscopy. TIRF microscopy provided ample time resolution and allowed for quick screening of large numbers of molecules at numerous lysine concentrations. Sample TIRF trajectories of donor (green), acceptor (red), and FRET efficiency (black) are demonstrated in Figure 5 for

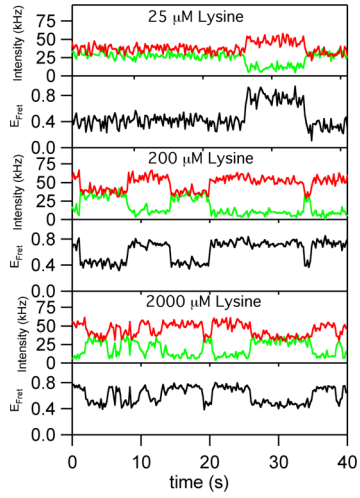

Figure 5. Representative time-resolved fluorescence intensity trajectories and corresponding FRET efficiencies from TIRF microscopy for the lysine riboswitch construct at 25, 200, and 2000 μM lysine conditions. The donor and acceptor intensities are plotted in green and red, respectively. The FRET efficiencies are plotted in black. Two E_{FRET} states are resolved at all lysine concentrations. The high E_{FRET} state (E_{FRET} = 0.75(3)) is assigned to a closed conformation that has bound lysine, and the low E_{FRET} state (E_{FRET} = 0.41(6)) is assigned to an opened conformation.

individual molecules under [lysine] = 25, 200, and 2000 μM conditions. Multiple examples of TIRF trajectories at numerous lysine concentrations have been included in Figures S5−S9 of the Supporting Information to demonstrate the heterogeneity observed within the trajectories. First of all, ≈30% of the molecules remain permanently open during the 2−500 s observation time, in agreement with the above-mentioned burst fluorescence and raster scanning studies. These molecules most likely represent inactive conformations of the ligand binding-pocket that prevent lysine binding and cannot be included in the analysis described in this section since they do not change FRET states on the time scale of these experiments. Of the remaining majority fraction (≈70%) of actively folding molecules under all lysine conditions, each molecule reveal FRET efficiency traces switching rapidly between 0.41(6) and 0.75(3) (see Figure 5). Most importantly, the distributions of dwell times for the open states are clearly affected by ligand concentration, with the molecule spending more time in the closed configuration at higher lysine concentrations.

In order to verify assignment of the high FRET state to a conformation in which the molecule closes after binding lysine, we have introduced a single-point mutation (G33C) to the lysine riboswitch construct. This mutation disrupts a critical base quadruple that inhibits lysine binding in the aptamer and results in a loss of transcriptional regulation.[7,39,44,45] If lysine binding is a necessary antecedent to conformational change, such a loss of lysine binding capability in our constructs should prevent conformational access to the high FRET state. By way of testing this hypothesis, Figure 6 displays representative confocal FRET traces at 1 mM lysine conditions for the wild-type *B. subtilis* lysine riboswitch construct (Figure 6a) and a G33C single-point mutation (Figure 6b). In excellent agree-

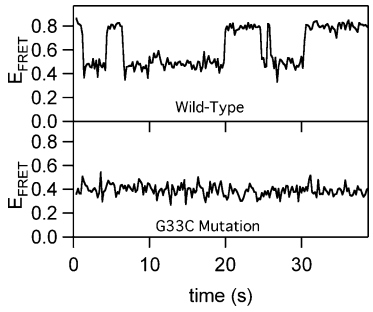

Figure 6. FRET efficiency traces from confocal trajectories at 1 mM lysine for the wild-type *B. subtilis* lysine riboswitch construct as shown in Figure 1 and for a lysine riboswitch construct with a single-point mutation (G33C). When the mutation is introduced, the riboswitch construct displays only one E_{FRET} state, corresponding to the conformation in which lysine is not bound to the aptamer domain.

ment with this hypothesis, the G33C mutant lysine riboswitch molecule in Figure 6 displays FRET efficiency traces containing only a single FRET state, with a low E_{FRET} value (0.41) consistent with the open conformation. Thus, we can conclude that (i) the E_{FRET} states at 0.41(6) and 0.75(3) in the wild-type construct represent the open and closed conformation, respectively, and (ii) lysine binding to the riboswitch is a necessary precursor step for accessing the closed conformation at physiological magnesium concentrations. It was observed earlier in the ensemble fluorescence measurements that the FRET state for the closed conformation could be achieved in the absence of ligand but only at high Mg^{2+} concentrations.

In addition, single molecule statistical analysis of the E_{FRET} trajectories can be performed to determine rate constants for both closing (k_{close}) and opening (k_{open}) of the riboswitch construct. To obtain these rate constants, we evaluate the cumulative distribution function (CDF), i.e., the running sum of the number of opening (or closing) events less than or equal to τ_{dwell}, as a function of τ_{dwell}. These CDFs contain the relevant statistics on cumulative time spent in either the closed or opened state and for a single rate process will be distributed with a characteristic exponential decay rate.[46] Sample CDFs for closing (right side panels) and opening (left side panels) events at 25, 200, and 2000 μM lysine are shown in Figure 7. Single-exponential fits to these cumulative distribution functions yield the observed rate constants k_{close} and k_{open} for closing and opening, respectively. It is immediately evident from Figure 7 that the opening rate constants are essentially independent of the lysine concentration and thus consistent with a simple, unimolecular elementary process. By way of contrast, the closing reaction exhibits a significant dependence on the lysine concentration, with k_{close} increasing systematically over the range of lysine concentrations sampled (25−2000 μM) and qualitatively more consistent with a bimolecular process.

To investigate this more quantitatively, the rate constants for closing and opening (k_{close} and k_{open}, respectively) have been plotted as a function of lysine concentration in Figure 8. As noted above, the opening rate constants (see Figure 8a) display essentially zero dependence on lysine concentration, with a simple average of all k_{open} values yielding 0.20(3) s^{-1}. The observed closing rate constant (see Figure 8b) shows a significant dependence to the lysine concentration, with k_{close} increasing 20-fold over the concentrations of lysine measured (25−2000 μM). The observed closing rate constant rises smoothly between 25 and 2000 μM lysine and reaches an

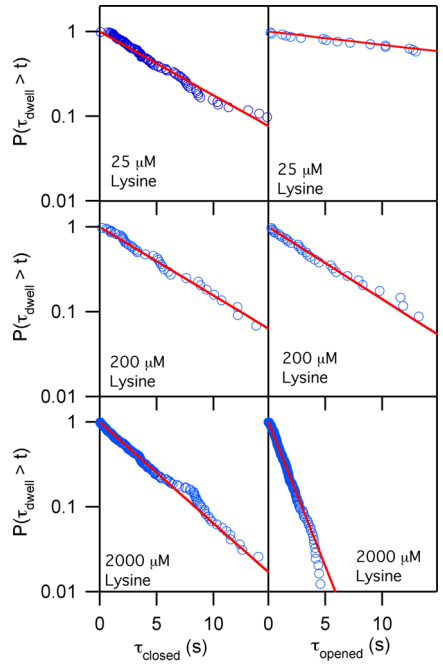

Figure 7. Cumulative distribution probabilities of the closed (left) and opened (right) dwell times for 25, 200, and 2000 μM lysine. The cumulative distribution plots are fit to single-exponential functions (solid red line) to determine the observed closing and opening rate constants.

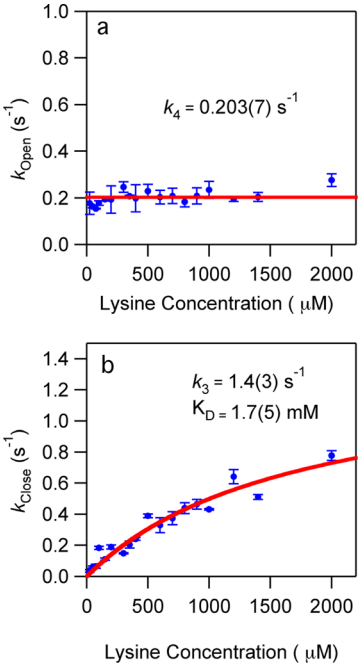

Figure 8. Lysine dependence of k_{open} (a) and k_{close} (b) of the riboswitch construct. k_{open} shows no dependence on lysine and is fit by a straight line with no slope (red line in (a)) to yield a rate of opening of 0.203(7) s^{-1}. The lysine dependence of k_{close} is fit by eq 5 (red line in (b)) to yield a rate of lysine induced folding (k_3) of 1.4(3) s^{-1} and a dissociation constant for lysine (K_D) of 1.7 (5) mM. This analysis reveals an apparent dissociation constant ($K_{D,apparent}$) for lysine equal to 0.25(9) mM.

asymptotic value under saturating lysine conditions. The present single-molecule trajectory analysis clearly demonstrates

dx.doi.org/10.1021/bi3007753 | *Biochemistry* 2012, 51, 9223−9233

that lysine accelerates the closing rate but does not seem to affect the opening rate constant. These observations are consistent with the folding kinetic model described by eq 4

$$\text{opened RNA} + \text{lysine} \underset{k_2}{\overset{k_1}{\rightleftarrows}} \text{opened RNA·lysine} \underset{k_4}{\overset{k_3}{\rightleftarrows}} \text{closed RNA·lysine} \quad (4)$$

where the two "open" RNA structures (lysine bound vs unbound) are not distinguished by the FRET measurement. The observed k_{open} values (see Figure 8a) are least-squares fit to a straight line with zero slope to obtain a rate constant of opening (k_4) of 0.203(7) s^{-1}.

Conversely, in the steady-state regime, the observed closing rate (k_{close}) from the model in eq 4 should depend on lysine concentration according to the Hill expression

$$k_{close} = \frac{k_3[\text{Lys}]^n}{K_D{}^n + [\text{Lys}]^n} \quad (5)$$

where k_3 is the elementary closing rate constant from the lysine bound state, $K_D = k_2/k_1$ is the dissociation constant for lysine binding, and n is a measure of any binding cooperativity. For a Hill coefficient fixed at unity, the data (see Figure 8b) can be well fit to eq 5 to yield a closing rate constant (k_3) of 1.4(3) s^{-1} and a dissociation constant for lysine binding (K_{D1}) of 1.7(5) mM. Note that K_{D1} is the true microscopic dissociation constant for ligand binding, which can differ from the apparent dissociation constant for binding and subsequent conformational change. As predicted from eq 4, this apparent dissociation constant is simply $K_{D,app} = K_{D1} \times K_{D2}$, with $K_{D1} = k_2/k_1$ and $K_{D2} = k_4/k_3 = 0.145(31)$. Since we measure k_3 and k_4 directly at the single molecule level, this analysis can be used to predict an effective dissociation constant for lysine binding of 1.7(5) mM × 0.145(31) = 0.25(9) mM, which is in excellent agreement with the apparent dissociation constant of $K_{D,app}$ = 0.23(2) mM measured using burst FRET methods. Since the apparent dissociation constants that are measure independently for freely diffusing molecules and surfaced tethered molecules are in excellent agreement with each other, we conclude that tethering of this riboswitch construct does not influence the kinetics of ligand binding. It is also worth noting that both single molecule measurements agree but differ slightly from the apparent dissociation constant measured via conventional ensemble fluorimetry methods, i.e., $K_{D,app}$ = 0.32(1) mM. One powerful advantage of the single-molecule verses ensemble methods is the use of alternating laser excitation (ALEX) methods, which can completely eliminate heterogeneous contributions from donor-only constructs and therefore arguably provides a more accurate measurement of the apparent dissociation constant.

Since the single molecule tethered trajectory data are consistent with the simple kinetic model in eq 4, further insight can be gleaned from the freely diffusing single molecule measurements. Specifically, we offered two hypotheses to explain why only a ≈ 58(2)% subset of the dually labeled constructs that diffuse through the confocal volume are actually closed under saturating lysine conditions. The first hypothesis is that a 42% subpopulation of molecules is trapped in an inactive conformation in which the ligand binding-pocket is misfolded. The second hypothesis is that a simple two-state model such as eq 1 is insufficient to describe the structural changes induced by lysine binding. At least three states are needed to describe the observed data. Indeed, the kinetics of the single molecule tethered trajectories clearly reveal that the second hypothesis is true. However, this interpretation would also suggest that the steady state fraction (α) of molecules closed after binding lysine should be $k_3/(k_3 + k_4)$ = 87(2)%. Since the fraction of molecules closed after lysine binding is even lower, only ≈58(2)%, this suggests that both hypotheses must be correct and that some misfolding is taking place. Indeed, this is qualitatively confirmed by the 28(4)% subset of molecules observed in the raster scanned images that do not appear to be capable of folding even under saturating lysine conditions. Therefore, our results reveal that there are molecules that do not fold even under saturating lysine conditions and that the simple two-state model in eq 1 is insufficient to describe the structural changes observed. A three-state model, as shown in eq 4, is needed to sufficiently explain the kinetics observed.

DISCUSSION

Riboswitches must undergo specific conformational changes upon ligand binding that influence the formation of secondary structures in the downstream expression platform. While chemical probing experiments have shown a structural rearrangement of the five-way helical junction of the lysine aptamer domain, previous small-angle X-ray scattering and crystallographic data have suggested that lysine binding has little effect on the global structure of the RNA.[25] Selective placement of our FRET pair, however, reveals that the P1 and P5 helices are reoriented by ligand induced folding of the five-way junction, as indicated by the lysine-dependent changes in FRET efficiency. The small-angle X-ray scattering and crystallographic data most likely did not observed the structural changes induced by lysine binding because these experiments were performed at elevated Mg^{2+} concentrations (10 mM). At these elevated Mg^{2+} concentrations the riboswitch is fully folded with or without ligand. Since P1 is directly involved in the secondary structural switch, the conformational changes that we observed at physiological Mg^{2+} concentrations are likely coupled to regulation. Our observations suggest that ligand binding cause the P1 and P5 helices to scissor into a closed conformation, indicated by the increase in FRET efficiency, providing a steric block to strand invasion by the expression platform and thus precluding formation of the competing antiterminator. The local folding rearrangements in the binding pocket of the lysine aptamer include formation of noncanonical A−G base pairs in the P1 helix to further stabilize this element against strand invasion.[7,25] Thus, coupling of (i) local folding transitions triggered by base pair formation with (ii) larger scale structural changes such as helical orientation may allow the RNA to generate a more robust regulatory response. Indeed, this model, whereby ligand binding causes the P1 and P5 helices to scissor into a closed conformation, is similar to behavior observed for the SAM-I riboswitch, for which the P1 and P3 axes are brought into a parallel orientation by binding of the SAM metabolite.[47,48]

Typically, a genetic regulatory feedback mechanism would be expected to be maximally responsive to intracellular concentration of the metabolite. However, previous measurements of the binding affinity for the lysine riboswitch have suggested that the *B. subtilis lysC* riboswitch binds lysine with 1−3 μM affinity,[7,26,49] i.e., 2−4 orders of magnitude below the 10^2−10^4 μM concentrations of free lysine reported in numerous bacterial species[20] as well as the 0.25(9) mM lysine binding affinity reported in this work. Interestingly the intracellular concentrations of many riboswitch ligands are in vast excess of the reported K_D's, suggesting that these RNAs would be poor

dx.doi.org/10.1021/bi3007753 | *Biochemistry* 2012, 51, 9223−9233

sensors for physiologically relevant concentration ranges. However, the short temporal windows available for ligand sensing imply that equilibrium binding is not always established during transcription and that the regulatory response is primarily governed by the kinetics of ligand binding rather than K_D. Direct evidence for kinetic control has been experimentally demonstrated for the FMN riboswitch and is implicated as a general feature of riboswitch regulation.[18] For example, the slow binding kinetics of the di-GMP riboswitches would suggest that the RNA would require μM concentrations of ligand to elicit regulation, as compared to the pM−nM binding affinities of the aptamer.[50] In contrast, the K_D of the lysine aptamer reported here, 0.25(9) mM, falls within the 10^2-10^4 μM concentrations of free lysine reported in numerous bacterial species,[20] suggesting that this RNA may be thermodynamically rather than kinetically controlled.

What is not yet taken into account is the sensitivity of the tertiary architecture of the RNA structure to the Mg^{2+} concentration, which can have profound consequences on the observed activity of functional RNAs.[51] Specifically, previous *in vitro* binding assays of the lysine riboswitch have been performed at magnesium concentrations of 10−20 mM, which is an order of magnitude higher than the typical concentration of Mg^{2+} present *in vivo* (0.5−1.5 mM)[20,52] and a very likely source of discrepancy between the current and earlier binding assays. These reports indicate that the lysine aptamer adopts a compact global fold at a $[Mg^{2+}]_{1/2}$ of 1.68 mM, suggesting that the riboswitch would be highly sensitive to the concentration of this cation.[49] By way of contrast, the data presented in this work argue that lysine binding to the riboswitch is as much as *2 orders of magnitude weaker* under physiologically relevant Mg^{2+} conditions, which would be consistent with a robust regulatory response under typical lysine concentrations found *in vivo*. However, additional studies will be required to understand the relationship between Mg^{2+}-dependent folding and lysine binding.

It is interesting to interpret magnitudes of the measured lysine binding and folding rate constant in terms of the desired biological function. First of all, the tethered single-molecule trajectory measurements performed in this work allow one to measure the microscopic dissociation constant for lysine binding (i.e., $K_{D2} = k_4/k_3$), as opposed to the apparent dissociation constant (i.e., $K_{D,app} = k_2/k_1 \times k_4/k_3$) obtained from ensemble studies. The 1.7(5) mM microscopic dissociation constant for lysine binding is in close agreement with the previously measured concentration of lysine required to elicit the half maximal regulatory response (T_{50}), 2.1(2) mM.[49] This observation supports the hypothesis that lysine binding establishes equilibrium quickly with respect to the subsequent closing process. Since the aptamer domain is synthesized first during transcription, this domain is therefore quickly able to sense its environment and achieve equilibrium between bound and unbound populations.

Second, in order to elicit the correct biological response, the riboswitch must subsequently close and stay closed during transcription of the expression platform. Given that the rate of transcription is ∼20−60 nucleotides per second[21] and the expression platform is ∼60 nucleotides, the aptamer domain has between 1.0 and 3.0 s to sense its environment, bind the ligand, and close. The absence of any fast double-exponential component in the cumulative distribution functions at short time scales indicates that achievement of the lysine binding equilibrium must be very fast relative to the closing and opening times. If the rate constants measured *in vitro* in this study approximate those in the cell, the characteristic $1/e$ dwell times for these closed and opened states would be 5.0 and 0.7 s, respectively. On the basis of these values, the aptamer domain would be able to successfully bind lysine and fold on a 0.7 s time scale comparable with and even shorter than nominally required to transcribe the expression platform. Furthermore, the 5.0 s dwell time for the closed conformation ensures that once the aptamer domain closes, it will remain closed for essentially the entire 1.0−3.0 s duration of the expression platform synthesis. Particularly in the context of the two-step kinetic model of eq 4, the observation that closing and opening time constants are comparable with or even faster than full transcription of the expression platform is quite interesting. Specifically, this implies that the regulatory response is controlled by the equilibrium distribution of lysine bound and unbound populations, rather than the kinetics of subsequent closing and opening events.

As a final comment, one interesting feature of the lysine riboswitch is its kinetic simplicity. Despite its relatively complex five-way junctional structure, ∼70% of the lysine riboswitch molecules observed appear to operate efficiently via achieving a fast equilibrium with lysine binding, followed by elementary closing and opening kinetics. Approximately 30% of the molecules do not appear to bind lysine on the time scale of the experiments. However, these molecules may represent a misfolded subpopulation due to annealing procedures used in the construct synthesis and may not represent a biologically relevant population. The majority of the molecules (∼70%) observed show a fast ligand binding equilibrium and elementary closing and opening kinetics, which is in contrast to many other functional RNAs. Many RNAs exhibit rough folding landscapes with many nonfunctional "native-like" intermediates that are significantly populated during folding/refolding of the RNA.[53−56] The apparently homogeneous nature of the lysine aptamer may reflect the selective pressure for riboswitches to rapidly form binding-active conformations in order to be able to productively bind their ligand during the short time scales of transcription. This view is consistent with observations that have been made for other riboswitch classes. For example, the SAM-I and adenine binding riboswitches both appear to behave primarily as two-state systems under physiological conditions.[48,57] However, both of these aptamers exhibit more complex folding behavior at lower Mg^{2+} concentrations due to loss of long-range tertiary interactions. The relevance of these observations to genetic regulation remains to be determined.

■ ASSOCIATED CONTENT

Ⓢ Supporting Information

Details pertaining to RNA synthesis, the experimental equipment used in this study, fluorescence techniques, and data analysis. This material is available free of charge via the Internet at http://pubs.acs.org.

■ AUTHOR INFORMATION

Corresponding Author

*E-mail: djn@jila.colorado.edu, Ph 303-492-8857.

Funding

Funding for this work was provided by a grant from the National Science Foundation and the Keck Foundation to D.J.N. L.R.F. acknowledges postdoctoral support from the National Research Council, R.T.B. acknowledges support by an

NIH grant (GM 073850), and A.D.G. acknowledges support from an NIH Biophysical Training Grant (T32 GM065103).

Notes

The authors declare no competing financial interest.

REFERENCES

(1) Mercer, T. R., Dinger, M. E., and Mattick, J. S. (2009) Long noncoding RNAs: insights into functions. *Nat. Rev. Genet. 10*, 155−159.
(2) Ketting, R. F. (2011) The many faces of RNAi. *Dev. Cell 20*, 148−161.
(3) Gripenland, J., Netterling, S., Loh, E., Tiensuu, T., Toledo-Arana, A., and Johansson, J. (2010) RNAs: regulators of bacterial virulence. *Nat. Rev. Microbiol. 8*, 857−866.
(4) Montange, R. K., and Batey, R. T. (2008) Riboswitches: emerging themes in RNA structure and function. *Annu. Rev. Biophys. 37*, 117−133.
(5) Roth, A., and Breaker, R. R. (2009) The structural and functional diversity of metabolite-binding riboswitches. *Annu. Rev. Biochem. 78*, 305−334.
(6) Mandal, M., Lee, M., Barrick, J. E., Weinberg, Z., Emilsson, G. M., Ruzzo, W. L., and Breaker, R. R. (2004) A glycine-dependent riboswitch that uses cooperative binding to control gene expression. *Science 306*, 275−279.
(7) Sudarsan, N., Wickiser, J. K., Nakamura, S., Ebert, M. S., and Breaker, R. R. (2003) An mRNA structure in bacteria that controls gene expression by binding lysine. *Genes Dev. 17*, 2688−2697.
(8) Dann, C. E., Wakeman, C. A., Sieling, C. L., Baker, S. C., Irnov, I., and Winkler, W. C. (2007) Structure and mechanism of a metal-sensing regulatory RNA. *Cell 130*, 878−892.
(9) Nahvi, A., Sudarsan, N., Ebert, M. S., Zou, X., Brown, K. L., and Breaker, R. R. (2002) Genetic control by a metabolite binding mRNA. *Chem. Biol. (Cambridge, MA, U. S.) 9*, 1043−1049.
(10) Winkler, W., Nahvi, A., and Breaker, R. R. (2002) Thiamine derivatives bind messenger RNAs directly to regulate bacterial gene expression. *Nature 419*, 952−956.
(11) Mandal, M., Boese, B., Barrick, J. E., Winkler, W. C., and Breaker, R. R. (2003) Riboswitches control fundamental biochemical pathways in bacillus subtilis and other bacteria. *Cell 113*, 577−586.
(12) Mandal, M., and Breaker, R. R. (2003) Adenine riboswitches and gene activation by disruption of a transcription termnator. *Nat. Struct. Mol. Biol. 11*, 29−35.
(13) Winkler, W. C., Nahvi, A., Roth, A., Collins, J. A., and Breaker, R. R. (2004) Control of gene expression by a natural metabolite-responsive ribozyme. *Nature 428*, 281−286.
(14) Irnov, Kertsburg, A., and Winkler, W. C. (2006) Genetic control by cis-acting regulatory RNAs in bacillus subtilis: general principles and prospects for discovery. *Cold Spring Harbor Symp. Quant. Biol. 71*, 239−249.
(15) Blount, K. F., and Breaker, R. R. (2006) Riboswitches as antibacterial drug targets. *Nat. Biotechnol. 24*, 1558−1564.
(16) Garst, A. D., and Batey, R. T. (2009) A switch in time: Detailing the life of a riboswitch. *Biochim. Biophys. Acta, Gene Regul. Mech. 1789*, 584−591.
(17) Winkler, W. C., and Breaker, R. R. (2003) Genetic control by metabolite binding riboswitches. *ChemBioChem 4*, 1024−1032.
(18) Wickiser, J. K., Winkler, W. C., Breaker, R. R., and Crothers, D. M. (2005) The speed of RNA transcription and metabolite binding kinetics operate an FMN riboswitch. *Mol. Cell 18*, 49−60.
(19) Greenleaf, W. J., Frieda, K. L., Foster, D. A. N., Woodside, M. T., and Block, S. M. (2008) Direct observation of hierarchical folding in single riboswitch aptamers. *Science 319*, 630−633.
(20) Bennett, B. D., Kimball, E. H., Gao, M., Osterhout, R., Van Dien, S. J., and Rabinowitz, J. D. (2009) Absolute metabolite concentrations and implied enzyme active site occupancy in *Escherichia coli*. *Nat. Chem. Biol. 5*, 593−599.
(21) Ardehali, M. B., and Lis, J. T. (2009) Tracking rates of transcription and splicing in vivo. *Nat. Struct. Mol. Biol. 16*, 1123−1124.
(22) Lemay, J. F., Desnoyers, G., Blouin, S., Heppell, B., Bastet, L., St-Pierre, P., Masse, E., and Lafontaine, D. A. (2011) Comparative study between transcriptionally- and translationally-acting adenine riboswitches reveals key differences in riboswitch regulatory mechanisms. *PLoS Genet. 7*, e1001278.
(23) Grundy, F. J., Lehman, S. C., and Henkin, T. M. (2003) The L box regulon: Lysine sensing by leader RNAs of bacterial lysine biosynthesis genes. *Proc. Natl. Acad. Sci. U. S. A. 100*, 12057−12062.
(24) Rodionov, D. A., Vitreschak, A. G., Mironov, A. A., and Gelfand, M. S. (2003) Regulation of lysine biosynthesis and transport genes in bacterial: yet another RNA riboswitch? *Nucleic Acids Res. 31*, 6748−6757.
(25) Garst, A. D., Heroux, A., Rambo, R. P., and Batey, R. T. (2008) Crystal structure of the lysine riboswitch regulatory mRNA element. *J. Biol. Chem. 283*, 22347−22351.
(26) Serganov, A., Huang, L., and Patel, D. J. (2008) Structural insights into amino acid binding and gene control by a lysine riboswitch. *Nature 455*, 1263−1267.
(27) Blouin, S., Chinnappan, R., and Lafontaine, D. A. (2011) Folding of the lysine riboswitch: importance of peripheral elements for transcriptional regulation. *Nucleic Acids Res. 39*, 3373−3387.
(28) Antonik, M., Felekyan, S., Gaiduk, A., and Seidel, C. A. M. (2006) Separating structural heterogeneities from stochastic variations in fluorescence resonance energy transfer distributions via photon distribution analysis. *J. Phys. Chem. B 110*, 6970−6978.
(29) Aitken, C. E., Marshall, R. A., and Puglisi, J. D. (2008) An oxygen scavenging system for improvement of dye stability in single-molecule fluorescence experiments. *Biophys. J. 94*, 1826−1835.
(30) Baird, N. J., and Ferre-D'Amare, A. R. (2010) Idiosyncratically tuned switching behavior of riboswitch aptamer domains revealed by comparative small-angle X-ray scattering analysis. *RNA 16*, 598−609.
(31) Batey, R. T., Gilbert, S. D., and Montange, R. K. (2004) Structure of a natural guanine-responsive riboswitch complexed with the metabolite hypoxanthine. *Nature 432*, 411−415.
(32) Edwards, A. L., Reyes, F. E., Heroux, A., and Batey, R. T. (2010) Structural basis for recognition of S-adenosylhomocysteine by riboswitches. *RNA 16*, 2144−2155.
(33) Kulshina, N., Edwards, T. E., and Ferre-D'Amare, A. R. (2010) Thermodynamic analysis of ligand binding and ligand binding-induced tertiary structure formation by the thiamine pyrophosphate riboswitch. *RNA 16*, 186−196.
(34) Cohen, S., and Burt, C. (1977) ^{31}P nuclear magnetic relaxation studies of phosphocreatine in intact muscle: determination of intracellular free magnesium. *Proc. Natl. Acad. Sci. U. S. A.*, 4271−4275.
(35) Mildvan, A. (1987) Role of magnesium and other divalent cations in ATP-utilizing enzymes. *Magnesium*, 28−33.
(36) Millart, H., Durlach, V., and Durlach, J. (1995) Red blood cell magnesium concentrations: analytical problems and significance. *Magnesium Res.*, 65−76.
(37) Uetani, T., Matsubara, T., Nomura, H., Murohara, T., and Nakayama, S. (2003) Ca^{2+}-dependent modulation of intracellular Mg^{2+} concentration with amiloride and KB-R7943 in pig carotid artery. *J. Biol. Chem.*, 47491−47497.
(38) Willcocks, J., Mulquiney, P., Ellory, J., Veech, R., Radda, G., and Clarke, K. (2002) Simultanewous determination of low free Mg^{2+} and pH in human sickle cells using ^{31}P NMR spectroscopy. *J. Biol. Chem.*, 49911−49920.
(39) Blount, K. F., Wang, J. X., Lim, J., Sudarsan, N., and Breaker, R. R. (2007) Antibacterial lysine analogs that target lysine riboswitches. *Nat. Chem. Biol. 3*, 44−49.
(40) Deniz, A. A., Dahan, M., Grunwell, J. R., Ha, T., Faulhaber, A. E., Chemla, D. S., Weiss, S., and Schultz, P. G. (1999) Single-pair fluorescence resonance energy transfer on freely diffusing molecules: Observation of Forster distance dependence and subpopulations. *Proc. Natl. Acad. Sci. U. S. A. 96*, 3670−3675.
(41) Deniz, A. A., Laurence, T. A., Dahan, M., Chemla, D. S., Schultz, P. G., and Weiss, S. (2001) Ratiometric single-molecule studies of freely diffusing biomolecules. *Annu. Rev. Phys. Chem. 52*, 233−253.

(42) Fiore, J. L., Hodak, J. H., Piestert, O., Downey, C. D., and Nesbitt, D. J. (2008) Monovalent and divalent promoted GAAA tetraloop-receptor tertiary interactions from freely diffusing single-molecule studies. *Biophys. J. 95*, 3892−3905.
(43) Hodak, J. H., Fiore, J. L., Nesbitt, D. J., Downey, C. D., and Pardi, A. (2005) Docking kinetics and equilibrium of a GAAA tetraloop-receptor motif probed by single-molecule FRET. *Proc. Natl. Acad. Sci. U. S. A. 102*, 10505−10510.
(44) Lu, Y., Shevtchenko, T. N., and Paulus, H. (1992) Fine-structure mapping of *cis*-acting control sites in the lysC operon of *Bacillus subtilis*. *FEMS Microbiol. Lett.*, 23−27.
(45) Vold, B., Szulmajster, J., and Carbone, A. (1975) Regulation of dihydrodipicolinate synthase and aspartate kinase in *Bacillus subtilis*. *J. Bacteriol.*, 970−974.
(46) Blanco, M., Walter, N. G., and Nils, G. W., in *Methods in Enzymology*, pp 153−178, Chapter 9, Academic Press, New York.
(47) Stoddard, C. D., Montange, R. K., Hennelly, S. P., Rambo, R. P., Sanbonmatsu, K. Y., and Batey, R. T. (2010) Free state conformational sampling of the SAM-I riboswitch aptamer domain. *Structure 18*, 787−797.
(48) Heppell, B., Blouin, S., Dussault, A.-M., Mulhbacher, J., Ennifar, E., Penedo, J. C., and Lafontaine, D. A. (2011) Molecular insights into the ligand-controlled organization of the SAM-I riboswitch. *Nat. Chem. Biol. 7*, 384−392.
(49) Blouin, S., and Lafontaine, D. A. (2007) A loop-loop interaction and a K-turn motif located in the lysine aptamer domain are important for the riboswitch gene regulation control. *RNA 13*, 1256−1267.
(50) Smith, K. D., Lipchock, S. V., Livingston, A. L., Shanahan, C. A., and Strobel, S. A. (2010) Structural and biochemical determinatnats of ligand binding by the c-di-GMP riboswitch. *Biochemistry 49*, 7351−7359.
(51) Carothers, J. M., Goler, J. A., Kapoor, Y., Lara, L., and Keasling, J. D. (2010) Selecting RNA aptamers for synthetic biology: investigating magnesium dependence and predicting binding affinity. *Nucleic Acids Res. 38*, 2736−2747.
(52) Tempest, D. W., Meers, J. L., and Brown, C. M. (1970) Influence of environment on the content and composition of microbial free amino acid pools. *J. Gen. Microbiol. 64*, 171−185.
(53) Solomatin, S. V., Greenfeld, M., Chu, S., and Herschlag, D. (2010) Multiple native states reveal persistent ruggedness of an RNA folding landscape. *Nature 463*, 681−686.
(54) Thirumalai, D., Klimov, D. K., and Woodson, S. A. (1997) Kinetic partitioning mechanism as a unifying theme in the folding of biomolecules. *Theor. Chem. Acc. 96*, 14−22.
(55) Treiber, D. K., and Williamson, J. R. (1999) Exposing the kinetic traps in RNA folding. *Curr. Opin. Struct. Biol. 9*, 339−345.
(56) Uhlenbeck, O. C. (1995) Keeping RNA happy. *RNA 1*, 4−6.
(57) Lemay, J. F., Penedo, J. C., Tremblay, R., Lilley, D. M. J., and Lafontaine, D. A. (2006) Folding of the adenine riboswitch. *Chem. Biol. (Cambridge, MA, U. S.) 13*, 857−868.
(58) Rasnik, I., McKinney, S. A., and Ha, T. (2006) Nonblinking and long-lasting single-molecule fluorescence imaging. *Nat. Methods 3*, 891−893.
(59) Gilbert, S. D., Stoddard, C. D., Wise, S. J., and Batey, R. T. (2006) Thermodynamic and kinetic characterization of ligand binding to the purine riboswitch aptamer domain. *J. Mol. Biol. 359*, 754−768.
(60) Kapanidis, A. N., Laurence, T. A., Lee, N. K., Margeat, E., Kong, X., and Weiss, S. (2005) Alternating-laser excitation of single molecules. *Acc. Chem. Res. 38*, 523−533.
(61) Kapanidis, A. N., Lee, N. K., Laurence, T. A., Doose, S. r., Margeat, E., and Weiss, S. (2004) Fluorescence-aided molecule sorting: Analysis of structure and interactions by alternating-laser excitation of single molecules. *Proc. Natl. Acad. Sci. U. S. A. 101*, 8936−8941.
(62) Lee, N. K., Kapanidis, A. N., Wang, Y., Michalet, X., Mukhopadhyay, J., Ebright, R. H., and Weiss, S. (2005) Accurate FRET measurements within single diffusing biomolecules using alternating-laser excitation. *Biophys. J. 88*, 2939−2953.
(63) Nir, E., Michalet, X., Hamadani, K. M., Laurence, T. A., Neuhauser, D., Kovchegov, Y., and Weiss, S. (2006) Shot-noise limited single-molecule FRET histograms: A comparison between theory and experiments. *J. Phys. Chem. B 110*, 22103−22124.
(64) Fries, J. R., Brand, L., Eggeling, C., Kollner, M., and Seidel, C. A. M. (1998) Quantitative identification of different single molecules by selective time-resolved confocal fluorescence spectroscopy. *J. Phys. Chem. A 102*, 6601−6613.
(65) Eigen, M., and Rigler, R. (1994) Sorting single molecules: application to diagnostics and evolutionary biotechnology. *Proc. Natl. Acad. Sci. U. S. A. 91*, 5740−5747.